Methane Activation

DOI: 10.1002/anie.201300900

Isomer-Selective Thermal Activation of Methane in the Gas Phase by $[HMO]^+$ and $[M(OH)]^+$ (M = Ti and V)**

*Robert Kretschmer, Maria Schlangen, and Helmut Schwarz**

Dedicated to Dr. Heike Schreer on the occasion of her 65th birthday

Transition-metal-catalyzed C–H bond-activation processes constitute an active area of research that has demonstrated repeatedly the enormous potential of catalytic organometallic chemistry.[1] Especially the activation and functionalization of methane has been identified as one of the key challenges in the context of addressing some aspects of the global energy problem.[2] While industrial processes under environmentally benign and economically feasible conditions have yet to be developed, the particular role of the electronic configuration of transition-metal complexes in the elementary steps of such bond-activation reactions have been addressed at quite some length.[3] Gas-phase studies provide an ideal arena to uncover mechanistic aspects in an unperturbed environment at a strictly molecular level.[4] While bare ground-state transition-metal ions of the first row do not bring about thermal C–H bond activation of CH_4,[5] the ligated Ni^{II} species $[NiD]^+$,[6] $[NiH]^+$,[7] and $[NiF]^+$[8] form the corresponding $[Ni(CH_3)]^+$ complexes [Equation (1)].

$$[Ni(L)]^+ + CH_4 \rightarrow [Ni(CH_3)]^+ + HL (L = D,H,F) \quad (1)$$

Furthermore, thermal activation of methane by 1) hydrogen-atom abstraction [Equation (2)],[4j] 2) dehydrogenation [Equation (3)], or 3) oxygen-atom transfer has been achieved by the first-row transition-metal oxide cations $[MO]^+$ with M = Mn–Cu.[9] The branching ratios of these three reactions are strongly affected by the electronic structures of $[MO]^+$.

$$[MO]^+ + CH_4 \rightarrow [M(OH)]^+ + CH_3 \quad (2)$$

$$[MO]^+ + CH_4 \rightarrow [M(CH_2)]^+ + H_2O \quad (3)$$

[*] Dr. R. Kretschmer, Dr. M. Schlangen, Prof. Dr. H. Schwarz
Institut für Chemie, Technische Universität Berlin
Strasse des 17. Juni 135, 10623 Berlin (Germany)
E-mail: Helmut.Schwarz@mail.chem.tu-berlin.de
Dr. R. Kretschmer
University of California San Diego
Department of Chemistry and Biochemistry
La Jolla, CA 92093-0343 (USA)

[**] Financial support from the Cluster of Excellence "Unifying Concepts in Catalysis" (EXC 314/1) funded by the Deutsche Forschungsgemeinschaft and administered by the Technische Universität Berlin is gratefully acknowledged. R.K. acknowledges the Stiftung Stipendien Fonds des Verbandes der Chemischen Industrie for a Kekulé scholarship and the Alexander von Humboldt Stiftung for a Feodor Lynen Research Fellowship. We thank the Institut für Mathematik der TU Berlin for the allocation of computer time.

Supporting information for this article is available on the WWW under http://dx.doi.org/10.1002/anie.201300900.

$$[MO]^+ + CH_4 \rightarrow [M]^+ + CH_3OH \quad (4)$$

Furthermore, bis-ligated 3d cations are also capable to activate methane, that is, $[CrO_2]^+$,[10] $[FeO(OH)]^+$,[11] and $[NiH(OH)]^+$,[12] reflecting the prominent role of the formal oxidation state of the metal. For example, $[Ni,O,H_2]^+$ serves as an interesting system demonstrating different reactivities of isomeric ions in gas-phase experiments. As expected, the Ni^I aqua complex $[Ni(H_2O)]^+$ does not react with methane [Equation (5)], while the corresponding Ni^{III} isomer, $[NiH(OH)]^+$, forms the ligand-exchange product $[Ni(CH_3)(OH)]^+$ accompanied by loss of H_2 [Equation (6)].[12]

$$[Ni(H_2O)]^+ + CH_4 \not\rightarrow \quad (5)$$

$$[NiH(OH)]^+ + CH_4 \rightarrow [Ni(CH_3)(OH)]^+ + H_2 \quad (6)$$

In contrast to these examples, which comprise middle and late first-row transition-metal complexes, methane activation by cationic complexes of Sc, Ti, and V has not been observed to date.[4g,h] Herein, we present studies about the C–H bond activation of methane by the isomeric species $[M(OH)]^+$ and $[HMO]^+$ with M = Ti, V in the formal oxidation states II and IV, respectively.[13] The corresponding ions have been generated in an electrospray ionization (ESI) source (for details, see the Methods Section) and investigated with a multipole-based mass spectrometer at room temperature.

Owing to the strong metal–oxygen bonds in $[MO]^+$[14] and $[M(OH)]^+$[15] and the less pronounced hydrogen-atom affinities (HAs) of $[MO]^+$ (M = Ti, V),[16] a distinction of $[M(OH)]^+$ and $[HMO]^+$ based on collision-induced dissociation (CID) experiments is not instructive because hydrogen-atom loss is expected for both species. To gain more structural information of these isomeric complexes, we performed parent-ion scans in which precursor ions can be identified. For the $[M,H,O]^+$ ions (M = Ti, V) formed from methanolic solutions of $TiCl_4$ and VCl_3, $[M,O_2,C,H_3]^+$ has been identified as a precursor. For this stoichiometry, three reasonable structural isomers are conceivable: 1) $[OM(OCH_3)]^+$ (**1**), 2) $[M(OH)(CH_2O)]^+$ (**2**), and 3) $[HMO(CH_2O)]^+$ (**3**). Energy-resolved CID experiments of $[M,O_2,C,H_3]^+$, for both M = Ti and V, result into two pronounced fragmentations with the elimination of neutral molecules of $\Delta m = 30$ and $\Delta m = 31$, corresponding to the eliminations of CH_2O and OCH_3, respectively (for details, see the Supporting Information, Figures S1, S2). While the loss of OCH_3 is indicative for $[OM(OCH_3)]^+$ (**1**), elimination of formaldehyde points to the existence of structures **2** and/or **3**. However, the loss of CH_2O prevails over that of OCH_3 at lower collision energies,

whereas the opposite behavior holds true at higher energies. These findings indicate that OCH_3 is eliminated by a direct entropically favored cleavage of the M–O bond while a more complex, less energy-demanding hydrogen shift from the methyl group in $[OM(OCH_3)]^+$ (**1**) to the oxo ligand or to the metal center, respectively, results in the formations of $[M(OH)(CH_2O)]^+$ (**2**) or $[HMO(CH_2O)]^+$ (**3**), respectively, and subsequent elimination of CH_2O. The generation of metal hydrides by a β-hydrogen shift constitutes a canonical process in the field of organometallic chemistry;[17] furthermore, it has been shown that this reaction plays a prominent role as well in the gas-phase chemistry of $[M(OCH_3)]^+$ species.[18] However, as demonstrated previously,[18d,19] a definitive distinction between $[M(OCH_3)]^+$ and $[HM(CH_2O)]^+$ using CID and neutralization-reionization experiments is not possible; this holds also true for the present system. Fortunately, computational studies can provide insight about the reaction pathways;[20] therefore, we calculated the two isomerization processes leading to $[M(OH)(CH_2O)]^+$ (**2**) and $[HMO(CH_2O)]^+$ (**3**) originating from $[OM(OCH_3)]^+$ (**1**); the potential-energy surfaces (PESs) are represented in Figure 1.

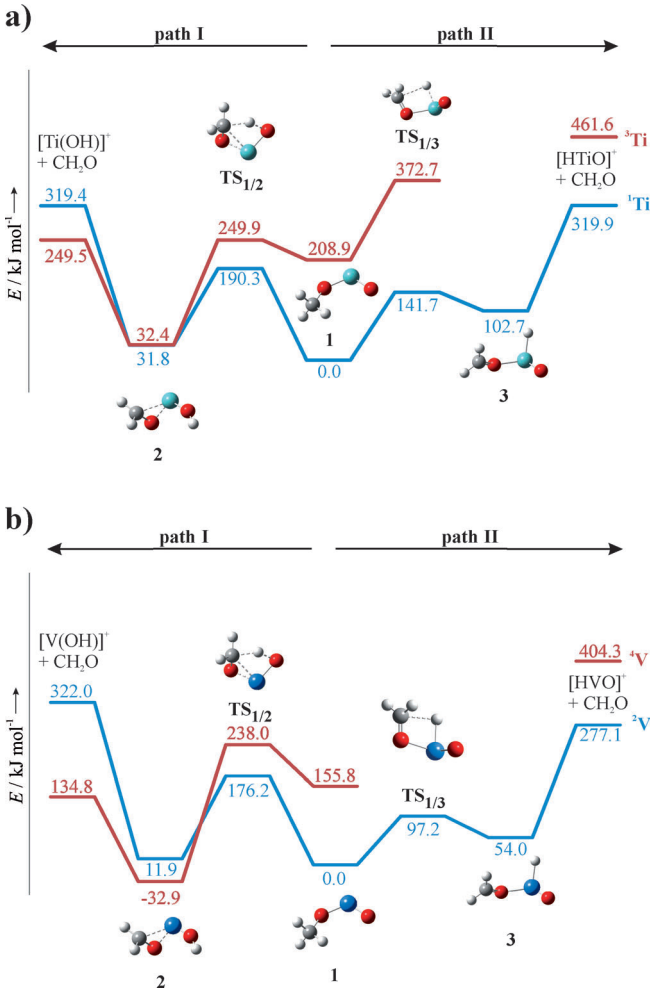

Figure 1. Potential-energy surfaces for the dissociation pathways of $[MO(OCH_3)]^+$ (1) with a) M = Ti and b) M = V for the low-spin (blue) and high-spin states (red). All energies are given in kJ mol^{-1}. Charges are omitted for the sake of clarity. C = dark gray, H = light gray, O = red, Ti = turquoise, V = blue; TS = transition state.

The energetic minima of the PESs differ for the two metal systems investigated. While for titanium the singlet state of $[OM(OCH_3)]^+$ (**1**) (M = Ti) corresponds to the global minimum, for vanadium the quartet state of $[M(OH)(CH_2O)]^+$ (**2**) is by 32.9 kJ mol^{-1} more stable compared to isomer **1** (M = V) in the doublet ground state. Starting from **1**, the hydrogen transfer can occur either as a γ-shift ($\mathbf{TS_{1/2}}$) leading to complex **2** (path I) or as a β-shift ($\mathbf{TS_{1/3}}$) resulting in the formation of $[HMO(CH_2O)]^+$ (**3**) (path II). The high-spin states of $\mathbf{TS_{1/2}}$ (M = Ti, V) and $\mathbf{TS_{1/3}}$ (M = Ti), given in red, are higher in energy compared to the respective low spin states (note that in the case of vanadium, the quartet state of $\mathbf{TS_{1/3}}$ could not be located on the PES); on the low-spin energy surfaces, for both metals $\mathbf{TS_{1/3}}$ requires less energy compared to $\mathbf{TS_{1/2}}$; thus, the formation of **3** is kinetically preferred by 48.6 kJ mol^{-1} and 79.0 kJ mol^{-1} for Ti and V, respectively. To generate the ground state product ion in path **1**→**2**→$[M(OH)]^+$ (M = Ti and V, path I, Figure 1), the operation of a two-state reactivity (TSR)[7,21] scenario is mandatory while this does not play a role for the formation of $[HMO]^+$ via **1**→**3**→$[HMO]^+$ (M = Ti and V, path II, Figure 1). Owing to the fact that spin-orbit coupling is less pronounced for first-row transition metals,[22] and especially for the early elements, a spin flip is not very likely to occur. Considering only the low-spin ground state of **1**, the thermochemical requirements for the formations of $[Ti(OH)]^+$ and $[HTiO]^+$ are more or less equal, that is, approximately equal amounts of $[Ti(OH)]^+$ and $[HTiO]^+$ should be formed in the experiments. For vanadium, however, the generation of $[HVO]^+$ is energetically favored by 44.9 kJ mol^{-1} compared to that of $[V(OH)]^+$, provided that no spin flip takes place to the quartet high-spin state. Finally, dissociations of **1** to $[TiO]^+$ and $[VO]^+$ accompanied by the loss of CH_3O [Equation (7)] require more energy compared

$$[OM(OCH_3)]^+ \rightarrow [MO]^+ + CH_3O \qquad (7)$$

to the other two dissociation pathways, that is, 377.2 kJ mol^{-1} (679.3 kJ mol^{-1}) and 427.5 kJ mol^{-1} (326.1 kJ mol^{-1}) relative to the entrance channel for Ti and V in their low (high) spin states, respectively, in line with the CID experiments.

For the specific formation of the $[M(OH)]^+$ isomers, alternative routes exist: While $[V(OH)]^+$ can easily be generated from an aqueous solution of VCl_3,[23] this method does not work for titanium because $TiCl_4$ in the presence of water immediately decomposes to insoluble TiO_2.[24] However, acidic solutions of Ti^{IV} ions react with hydrogen peroxide to the yellow $[Ti(O_2)(OH)]^+$ complex, in which the O_2 moiety binds side-on to the metal center;[24] thus, $[Ti(OH)]^+$ is accessible by the evaporation of weakly bound O_2 in the course of the ESI process. Here, the co-generation of $[HMO]^+$ (M = Ti, V) does not take place as indicated by the finding that the $[M,H,O]^+$ ion generated under these conditions is not reactive towards methane, which is discussed in the following.

The so-formed ions have then been allowed to react with methane under thermal conditions, as exemplified in Figure 2 for $[Ti(OH)]^+$ and $[HTiO]^+$. For both $[M(OH)]^+/CH_4$ couples (M = Ti, V) no reactions with CH_4 have been observed at the detection limit, in line with the known thermodynamic

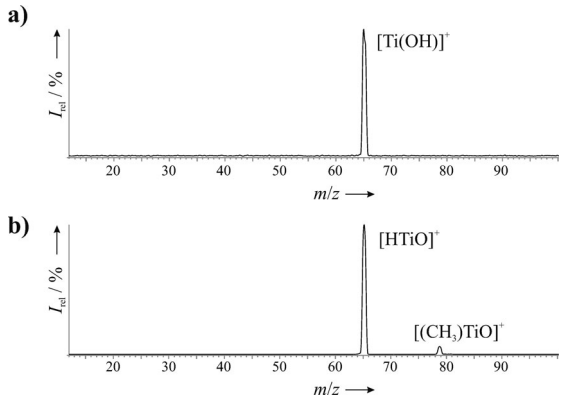

Figure 2. Ion/molecule reactions of mass-selected a) $[Ti(OH)]^+$ and b) $[HTiO]^+$ with methane ($p = 3.6 \times 10^{-4}$ mbar). Similar spectra are obtained for $[V(OH)]^+$ and $[HVO]^+$, respectively (for details, see the Supporting Information, Figure S3).

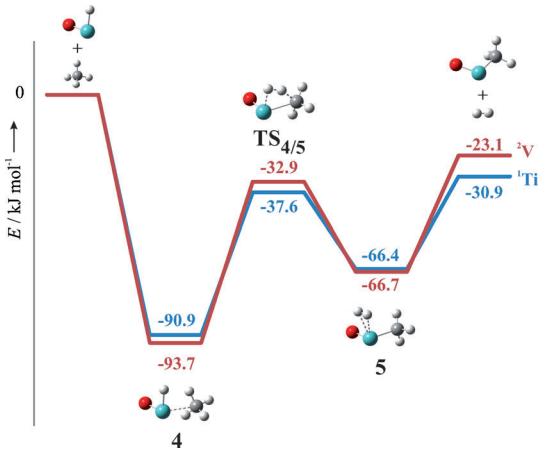

Figure 3. Potential-energy surfaces of the reactions of $[HTiO]^+$ (singlet state, blue) and $[HVO]^+$ (doublet state, red) with methane. All energies are given in kJ mol^{-1}. Charges are omitted for the sake of clarity. C = dark gray, H = light gray, O = red, M = turquoise.

parameters.[15,25] In contrast, reaction of $[HMO]^+$ with methane leads to the corresponding $[(CH_3)MO]^+$ ions accompanied by loss of H_2. The rate constants for these ligand-exchange reactions amount to 1.5×10^{-10} cm^{-3} s^{-1} molecule^{-1} and 1.1×10^{-10} cm^{-3} s^{-1} molecule^{-1} for $[HTiO]^+$ and $[HVO]^+$, respectively;[26] these values correspond to efficiencies of 15% and 11% relative to the gas-kinetic collision limit.[27] However, these data are lower limits owing to the overlap of isobaric $[HMO]^+$ with unreactive $[M(OH)]^+$, which is concomitantly generated from methanolic solutions (see above).

The assignment of the ligand exchange to generate molecular hydrogen is in keeping with labeling experiments, in which CD_4 and CH_2D_2 have been employed; intramolecular kinetic isotope effects (KIEs) of 1.8 (Ti) and 1.4 (V) are observed for the $[HMO]^+/CH_2D_2$ couples, respectively. Furthermore, very minor signals (< 1%) that are due to an inefficient H/D exchange of the hydrido ligand with the incoming deuterium-labeled hydrocarbon [Equation (8)] are observed.

$$[HMO]^+ + CD_4 \rightarrow [DMO]^+ + CHD_3 \qquad (8)$$

DFT calculations were performed to obtain mechanistic insight in the C–H bond-activation process, as well as to the origin of the non-occurrence of the methane activation by $[M(OH)]^+$. Figure 3 shows the PESs of the low-spin ground states (that is, ^{1}Ti and ^{2}V); note that the related high-spin states (^{3}Ti and ^{4}V), are much higher in energy ($^3[HTiO]^+$ 141.7 kJ mol^{-1}, $^4[HVO]^+$ 127.2 kJ mol^{-1}) such that they do not need to be considered for thermal or quasi-thermal reactions. In the first step, the $[HMO]^+$ ions and CH_4 form the encounter complex $[HMO(CH_4)]^+$ (**4**) with nearly identical exothermicities for both M = Ti and V, that is, −90.9 kJ mol^{-1} and −93.7 kJ mol^{-1}, respectively. Next, a hydrogen atom from methane is transferred to the hydride ligand in a concerted manner, that is, cleavage of M–H and C–H bonds and the formation of H–H and M–C bonds take place simultaneously via transition structure $\mathbf{TS_{4/5}}$, thus generating in a σ-bond metathesis process intermediate $[(CH_3)MO(H_2)]^+$ (**5**). The relatively weakly bound H_2 is easily evaporated from intermediate **5** to give rise to the corresponding $[(CH_3)MO]^+$ complexes; the overall thermochemistry is by 7.8 kJ mol^{-1} more favored for titanium compared to vanadium, in agreement with the experimental results.

Furthermore, the M–O bond lengths in going from $[HMO]^+$ to $[(CH_3)MO(H_2)]^+$ (**5**) remain unchanged; $d_{M\text{-}O}$ corresponds to 1.57 Å for Ti and 1.54 Å for V for both species, respectively, and only in the formation of the product ion $[(CH_3)MO]^+$ a minor elongation of 0.1 Å takes place. As the barrier $\mathbf{TS_{4/5}}$ is located below the exit channel, the observed H/D scrambling [Equation (8)] finds an obvious explanation. Other conceivable processes, for example, H-atom abstraction by the oxygen center can be ruled out; this step has been calculated to be endothermic by 380.3 kJ mol^{-1} (190.3 kJ mol^{-1}) and 256.3 kJ mol^{-1} (372.3 kJ mol^{-1}) for both metals in their high (low) spin states. Although the oxygen atom of $[HMO]^+$ is not directly involved in the bond breaking and making and thus may be viewed as an innocent spectator ligand, its presence is necessary to achieve the activation of methane under thermal conditions; this process is endothermic for the corresponding $[MH]^+/CH_4$ couples [Equation (9)]

$$[MH]^+ (M = Ti,V) + CH_4 \not\rightarrow [M(CH_3)]^+ + H_2 \qquad (9)$$

according to reported bond-dissociation energies (BDEs).[25b,28] In contrast, according to the calculations, both the M–H and M–CH_3 bonds in $[HMO]^+$ and $[(CH_3)MO]^+$ are weakened by the oxo ligand compared to $[MH]^+$ and $[M(CH_3)]^+$, respectively. However, this effect is more pronounced for $[HMO]^+$ than for $[(CH_3)MO]^+$; BDE(OM^+–H) is decreased by 63.5 kJ mol^{-1} and 54.5 kJ mol^{-1} compared to BDE(M^+–H) for M = Ti and V, respectively, while BDE(OM^+–CH_3) is lowered by only 45.6 kJ mol^{-1} (Ti) and 5.6 kJ mol^{-1} (V) in comparison to BDE(M^+–CH_3). This is also reflected in the M–H bonding orbitals: According to the natural bond orbital (NBO) analysis,[29] the electron density of the 4s orbital is reduced for $[HMO]^+$ (Ti: 22.4%, V: 22.8%) compared to that for $[MH]^+$ (Ti: 38.8%, V: 29.4%), thus

making the diffuse 4s orbital more available as electron acceptor of the C–H bond of methane in transition structure $\mathbf{TS_{4/5}}$.[7a]

Finally, the non-occurrence of the C–H bond activation in the $[M(OH)]^+/CH_4$ couples is not only the result of an unfavorable thermochemistry, as shown earlier by comparing the bond-dissociation energies,[15,25] also a kinetic barrier (57.8 kJ mol^{-1} and 72.6 kJ mol^{-1} for the high-spin ground states of Ti and V, respectively) prevents the formation of $[M(CH_3)]^+$ and H_2O under thermal or quasi thermal conditions.

In summary, in this combined experimental/theoretical study we present the first example of methane activation by early first-row transition-metal cations and highlight the crucial role of oxygen as a seemingly innocent spectator ligand in the course of the ligand-exchange process. While the $[MH]^+$ and $[M(OH)]^+$ ions (M = Ti, V) do not react with methane [Equations (9) and (10)], the isomeric $[HMO]^+$ species are able to bring about C–H bond activation of methane [Equation (11)].

$$[M(OH)]^+(M = Ti,V) + CH_4 \not\rightarrow \quad (10)$$

$$[HMO]^+(M = Ti, V) + CH_4 \rightarrow [(CH_3)MO]^+ + H_2 \quad (11)$$

Methods

The experiments were performed with a VG BIO-Q mass spectrometer of QHQ configuration (Q: quadrupole, H: hexapole) equipped with an ESI source as described in detail before.[30] Millimolar solutions of $TiCl_4$ and VCl_3 in pure methanol, VCl_3 in water, or $TiO(SO_4)$ in H_2O/H_2O_2 were introduced through a fused-silica capillary to the ESI source by a syringe pump (ca. 4 μL min^{-1}) to produce the metal-complex cations. Nitrogen was used as a nebulizing and drying gas at a source temperature of 80 °C. Maximal yields of the desired complexes were achieved by adjusting the cone voltage (U_c) between 70 and 80 V; U_c determines the degree of collisional activation of the incident ions in the transfer from the ESI source to the mass spectrometer. The identity of the ions was confirmed by comparison with the expected isotope patterns.[31] The ion/molecule reactions of the complexes with the substrates were probed at a collision energy (E_{lab}) set to nominally 0 eV, which in conjunction with the ca. 0.4 eV kinetic energy width of the parent ion at peak half height allows the investigation of quasi thermal reactions, as demonstrated previously.[20c,32]

Calculations were performed with the Gaussian 09 program package[33] using def2-QZVP basis sets[34] and the unrestricted B3LYP level of theory;[35] in a comparative study of $[M\text{-}OH_n]^+$ (n = 0–2) using 8 different DFT functionals, B3LYP was found to perform best regarding accuracy and error distribution.[16] Furthermore, the energy gap between $[Ti(OH)]^+$ and $[HTiO]^+$ (ΔE = 70.4 kJ mol^{-1}) is in good agreement with results obtained from MRCI calculations (ΔE = 68.2 kJ mol^{-1}).[36] To verify stationary points and transition states, frequency calculations were performed. All energies (given in kJ mol^{-1}) are corrected for (unscaled) zero-point vibrational energy contributions. Intrinsic reaction coordinate (IRC) calculations were performed to link transition structures with the corresponding minima.[37]

Received: February 1, 2013
Published online: April 25, 2013

Keywords: C–H activation · gas-phase reactions · ligand effects · metal complexes · oxidation states

[1] a) B. L. Conley, W. J. Tenn, K. J. H. Young, S. Ganesh, S. Meier, V. Ziatdinov, O. Mironov, J. Oxgaard, J. Gonzales, W. A. Goddard, R. A. Periana, *Methane Functionalization*, Wiley-VCH, Weinheim, **2006**; b) W. B. Tolman, *Activation of Small Molecules*: *Organometallic and Bioinorganic Perspectives*, Wiley-VCH, Weinheim, **2006**.

[2] a) J. R. Webb, T. Bolano, T. B. Gunnoe, *ChemSusChem* **2011**, *4*, 37–49; b) G. A. Olah, A. Goeppert, G. K. S. Prakash, *Beyond Oil and Gas*: *The Methanol Economy*, Wiley-VCH, Weinheim, **2009**; c) G. A. Olah, *Angew. Chem.* **2013**, *125*, 112–116; *Angew. Chem. Int. Ed.* **2013**, *52*, 104–107.

[3] a) A. E. Shilov, G. B. Shul′pin, *Chem. Rev.* **1997**, *97*, 2879–2932; b) S. S. Stahl, J. A. Labinger, J. E. Bercaw, *Angew. Chem.* **1998**, *110*, 2298–2311; *Angew. Chem. Int. Ed.* **1998**, *37*, 2180–2192; c) C. G. Jia, T. Kitamura, Y. Fujiwara, *Acc. Chem. Res.* **2001**, *34*, 633–639; d) J. A. Labinger, J. E. Bercaw, *Nature* **2002**, *417*, 507–514; e) R. H. Crabtree, *J. Organomet. Chem.* **2004**, *689*, 4083–4091; f) K. Godula, D. Sames, *Science* **2006**, *312*, 67–72; g) R. G. Bergman, *Nature* **2007**, *446*, 391–393; h) H. M. L. Davies, J. R. Manning, *Nature* **2008**, *451*, 417–424; i) Y. Boutadla, D. L. Davies, S. A. Macgregor, A. I. Poblador-Bahamonde, *Dalton Trans.* **2009**, 5820–5831; j) G. B. Shul'pin, *Org. Biomol. Chem.* **2010**, *8*, 4217–4228; k) the whole issue of *Chem. Rev.* **2010**, *110*, 575 has been dedicated to the topic of selective C–H bond activation; l) T. Newhouse, P. S. Baran, *Angew. Chem.* **2011**, *123*, 3422–3435; *Angew. Chem. Int. Ed.* **2011**, *50*, 3362–3374.

[4] a) K. Eller, H. Schwarz, *Chem. Rev.* **1991**, *91*, 1121–1177; b) D. K. Böhme, H. Schwarz, *Angew. Chem.* **2005**, *117*, 2388–2406; *Angew. Chem. Int. Ed.* **2005**, *44*, 2336–2354; c) D. K. Böhme, *Can. J. Chem.* **2008**, *86*, 177–198; d) G. E. Johnson, E. C. Tyo, A. W. Castleman, Jr., *Proc. Natl. Acad. Sci. USA* **2008**, *105*, 18108–18113; e) J. Roithová, D. Schröder, *Coord. Chem. Rev.* **2009**, *253*, 666–677; f) M. Schlangen, H. Schwarz, *Dalton Trans.* **2009**, 10155–10165; g) J. Roithová, D. Schröder, *Chem. Rev.* **2010**, *110*, 1170–1211; h) H. Schwarz, *Angew. Chem.* **2011**, *123*, 10276–10297; *Angew. Chem. Int. Ed.* **2011**, *50*, 10096–10115; i) R. Kretschmer, M. Schlangen, H. Schwarz, *Chem. Eur. J.* **2012**, *18*, 40–49; j) N. Dietl, M. Schlangen, H. Schwarz, *Angew. Chem.* **2012**, *124*, 5638–5650; *Angew. Chem. Int. Ed.* **2012**, *51*, 5544–5555.

[5] a) P. B. Armentrout, J. L. Beauchamp, *Acc. Chem. Res.* **1989**, *22*, 315–321; b) J. C. Weisshaar, *Acc. Chem. Res.* **1993**, *26*, 213–219; c) P. B. Armentrout, *Acc. Chem. Res.* **1995**, *28*, 430–436; d) H. Schwarz, D. Schröder, *Pure Appl. Chem.* **2000**, *72*, 2319–2332.

[6] T. J. Carlin, L. Sallans, C. J. Cassady, D. B. Jacobson, B. S. Freiser, *J. Am. Chem. Soc.* **1983**, *105*, 6320–6321.

[7] a) Q. Zhang, M. T. Bowers, *J. Phys. Chem. A* **2004**, *108*, 9755–9761; b) M. Schlangen, H. Schwarz, *Angew. Chem.* **2007**, *119*, 5711–5715; *Angew. Chem. Int. Ed.* **2007**, *46*, 5614–5617.

[8] M. Schlangen, H. Schwarz, *Helv. Chim. Acta* **2008**, *91*, 2203–2210.

[9] a) D. Schröder, H. Schwarz, *Angew. Chem.* **1990**, *102*, 1468–1469; *Angew. Chem. Int. Ed. Engl.* **1990**, *29*, 1433–1434; b) M. F. Ryan, A. Fiedler, D. Schroeder, H. Schwarz, *Organometallics* **1994**, *13*, 4072–4081; c) Y.-M. Chen, D. E. Clemmer, P. B. Armentrout, *J. Am. Chem. Soc.* **1994**, *116*, 7815–7826; d) M. F. Ryan, A. Fiedler, D. Schröder, H. Schwarz, *J. Am. Chem. Soc.* **1995**, *117*, 2033–2040; e) D. Schröder, H. Schwarz, *Angew. Chem.* **1995**, *107*, 2126–2150; *Angew. Chem. Int. Ed. Engl.* **1995**, *34*, 1973–1995; f) D. Schröder, H. Schwarz, D. E. Clemmer, Y. Chen, P. B. Armentrout, V. I. Baranov, D. K. Böhme, *Int. J. Mass. Spectrom. Ion Processes* **1997**, *161*, 175–191; g) N. Dietl, C. van der Linde, M. Schlangen, M. K. Beyer, H. Schwarz, *Angew. Chem.* **2011**, *123*, 5068–5072; *Angew. Chem. Int. Ed.* **2011**, *50*, 4966–4969.

[10] A. Fiedler, I. Kretzschmar, D. Schroder, H. Schwarz, *J. Am. Chem. Soc.* **1996**, *118*, 9941 – 9952.

[11] D. Schröder, H. Schwarz, *Angew. Chem.* **1991**, *103*, 987 – 989; *Angew. Chem. Int. Ed. Engl.* **1991**, *30*, 991 – 993.

[12] a) M. Schlangen, D. Schröder, H. Schwarz, *Angew. Chem.* **2007**, *119*, 1667 – 1671; *Angew. Chem. Int. Ed.* **2007**, *46*, 1641 – 1644; b) O. Lakuntza, J. M. Matxain, F. Ruiperez, M. Besora, F. Maseras, J. M. Ugalde, M. Schlangen, H. Schwarz, *Phys. Chem. Chem. Phys.* **2012**, *14*, 9306 – 9310; c) high-level electronic structure calculations have revealed that $[NiH(OH)]^+$ is better described as a $(H)Ni^{II}–(OH)^{\bullet}$ rather than a $(H)Ni^{III}–(OH)^-$ species: Y. Dede, X. Zhang, M. Schlangen, H. Schwarz, M.-H. Baik, *J. Am. Chem. Soc.* **2009**, *131*, 12634 – 12642.

[13] The Mulliken atomic spin-density distribution for both $[M(OH)]^+$ and $[HMO]^+$ (M = Ti,V), is consistent with the assigned formal oxidations states II and IV, respectively.

[14] a) E. R. Fisher, J. L. Elkind, D. E. Clemmer, R. Georgiadis, S. K. Loh, N. Aristov, L. S. Sunderlin, P. B. Armentrout, *J. Chem. Phys.* **1990**, *93*, 2676 – 2691; b) D. E. Clemmer, J. L. Elkind, N. Aristov, P. B. Armentrout, *J. Chem. Phys.* **1991**, *95*, 3387 – 3393.

[15] D. E. Clemmer, N. Aristov, P. B. Armentrout, *J. Phys. Chem.* **1993**, *97*, 544 – 552.

[16] X. H. Zhang, H. Schwarz, *Theor. Chem. Acc.* **2011**, *129*, 389 – 399.

[17] a) C. Elschenbroich, *Organometallchemie*, *5. ed.*, B. G. Teubner, Wiesbaden, **2005**; b) *Organotransition Metal Chemistry*: *From Bonding to Catalysis* (Ed.: J. F. Hartwig), University Science Book, Sausalito, **2010**.

[18] a) R. Houriet, L. F. Halle, J. L. Beauchamp, *Organometallics* **1983**, *2*, 1818 – 1829; b) G. Czekay, T. Drewello, H. Schwarz, *J. Am. Chem. Soc.* **1989**, *111*, 4561 – 4563; c) G. Czekay, T. Drewello, K. Eller, W. Zummack, H. Schwarz, *Organometallics* **1989**, *8*, 2439 – 2446; d) A. Fiedler, D. Schröder, H. Schwarz, B. L. Tjelta, P. B. Armentrout, *J. Am. Chem. Soc.* **1996**, *118*, 5047 – 5055; e) D. Schröder, H. Schwarz, S. Polarz, M. Driess, *Phys. Chem. Chem. Phys.* **2005**, *7*, 1049 – 1053; f) P. Gruene, C. Trage, D. Schröder, H. Schwarz, *Eur. J. Inorg. Chem.* **2006**, 4546 – 4552; g) M. Schlangen, H. Schwarz, *ChemCatChem* **2010**, *2*, 799 – 802.

[19] C. J. Cassady, B. S. Freiser, *J. Am. Chem. Soc.* **1985**, *107*, 1566 – 1573.

[20] a) S. Niu, M. B. Hall, *Chem. Rev.* **2000**, *100*, 353 – 406; b) A. J. Bell, A. Citra, J. M. Dyke, F. Ferrante, L. Gagliardi, P. Watts, *Phys. Chem. Chem. Phys.* **2004**, *6*, 1213 – 1218; c) D. Schröder, M. Engeser, H. Schwarz, E. C. E. Rosenthal, J. Döbler, J. Sauer, *Inorg. Chem.* **2006**, *45*, 6235 – 6245.

[21] D. Schröder, S. Shaik, H. Schwarz, *Acc. Chem. Res.* **2000**, *33*, 139 – 145.

[22] a) M. Blume, R. E. Watson, *Proc. R. Soc. London Ser. A* **1962**, *270*, 127 – 143; b) G. M. Cole, B. B. Garrett, *Inorg. Chem.* **1970**, *9*, 1898 – 1902; c) M. Vijayakumar, M. S. Gopinathan, *J. Mol. Struct. THEOCHEM* **1996**, *361*, 15 – 19.

[23] a) Z. Cheng, K. Siu, R. Guevremont, S. Berman, *J. Am. Soc. Mass Spectrom.* **1992**, *3*, 281 – 288; b) D. Vukomanovic, J. A. Stone, *Int. J. Mass Spectrom.* **2000**, *202*, 251 – 259; c) M. K. Beyer, *Mass Spectrom. Rev.* **2007**, *26*, 517 – 541.

[24] A. F. Holleman, E. Wiberg, *Lehrbuch der Anorganischen Chemie*, *101 ed.*, Walter de Gruyter, Berlin, **1995**.

[25] a) P. B. Armentrout, R. Georgiadis, *Polyhedron* **1988**, *7*, 1573 – 1581; b) *Organometallic Ion Chemistry* (Ed.: B. S. Freiser), Kluwer, Dordrecht, **1996**.

[26] The absolute rate coefficient for the reaction cannot be measured directly in our multipole setup; rather, the rate coefficient was determined by using the $[Pt]^+/CH_4$ system as a reference: D. Schröder, H. Schwarz, *Can. J. Chem.* **2005**, *83*, 1936 – 1940, and references cited therein.

[27] Collision-rate calculations (G. Gioumousis, D. P. Stevenson, *J. Chem. Phys.* **1958**, *29*, 294 – 299) were performed by using the following method: M. P. Langevin, *Ann. Chim. Phys.* **1905**, *8*, 245 – 288.

[28] a) J. L. Elkind, P. B. Armentrout, *Int. J. Mass. Spectrom. Ion Processes* **1988**, *83*, 259 – 284; b) J. L. Elkind, P. B. Armentrout, *J. Phys. Chem.* **1985**, *89*, 5626 – 5636.

[29] F. Weinhold, C. R. Landis, *Discovering Chemistry with Natural Bond Orbitals*, Wiley, Hoboken, **2012**.

[30] C. Trage, D. Schröder, H. Schwarz, *Chem. Eur. J.* **2005**, *11*, 619 – 627.

[31] Scientific Instrument Services: Isotope Distribution Calculator and Mass Spec Plotter. http://www.sisweb.com/mstools/isotope.html.

[32] a) D. Schröder, H. Schwarz, S. Schenk, E. Anders, *Angew. Chem.* **2003**, *115*, 5241 – 5244; *Angew. Chem. Int. Ed.* **2003**, *42*, 5087 – 5090; b) C. Trage, M. Diefenbach, D. Schröder, H. Schwarz, *Chem. Eur. J.* **2006**, *12*, 2454 – 2464.

[33] Gaussian 09 (Revision A.1), M. J. Frisch, G. W. Trucks, H. B. Schlegel, G. E. Scuseria, M. A. Robb, J. R. Cheeseman, G. Scalmani, V. Barone, B. Mennucci, G. A. Petersson, H. Nakatsuji, M. Caricato, X. Li, H. P. Hratchian, A. F. Izmaylov, J. Bloino, G. Zheng, J. L. Sonnenberg, M. Hada, M. Ehara, K. Toyota, R. Fukuda, J. Hasegawa, M. Ishida, T. Nakajima, Y. Honda, O. Kitao, H. Nakai, T. Vreven, J. Montgomery, J. A., J. E. Peralta, F. Ogliaro, M. Bearpark, J. J. Heyd, E. Brothers, K. N. Kudin, V. N. Staroverov, R. Kobayashi, J. Normand, K. Raghavachari, A. Rendell, J. C. Burant, S. S. Iyengar, J. Tomasi, M. Cossi, N. Rega, N. J. Millam, M. Klene, J. E. Knox, J. B. Cross, V. Bakken, C. Adamo, J. Jaramillo, R. Gomperts, R. E. Stratmann, O. Yazyev, A. J. Austin, R. Cammi, C. Pomelli, J. W. Ochterski, R. L. Martin, K. Morokuma, V. G. Zakrzewski, G. A. Voth, P. Salvador, J. J. Dannenberg, S. Dapprich, A. D. Daniels, Ö. Farkas, J. B. Foresman, J. V. Ortiz, J. Cioslowski, D. J. Fox, Gaussian Inc. Wallingford CT, **2009**.

[34] F. Weigend, R. Ahlrichs, *Phys. Chem. Chem. Phys.* **2005**, *7*, 3297 – 3305.

[35] a) C. Lee, W. Yang, R. G. Parr, *Phys. Rev. B* **1988**, *37*, 785 – 789; b) A. D. Becke, *J. Chem. Phys.* **1993**, *98*, 5648 – 5652.

[36] E. Miliordos, J. F. Harrison, K. L. C. Hunt, *J. Chem. Phys.* **2011**, *135*, 144111.

[37] a) K. Fukui, *J. Phys. Chem.* **1970**, *74*, 4161 – 4163; b) K. Fukui, *Acc. Chem. Res.* **1981**, *14*, 363 – 368; c) C. Gonzalez, H. B. Schlegel, *J. Phys. Chem.* **1990**, *94*, 5523 – 5527; d) D. G. Truhlar, M. S. Gordon, *Science* **1990**, *249*, 491 – 498.

